Single and Dual-Band Microstrip Patch Antennas for mm-Wave 5G Connectivity

Khalid[1], Dr. Seeta Ram Jalandhara[2]

[1] *Electronics & Communication Engineering, Maulana Azad University, Jodhpur, India*

[2] *Electronics & Communication Engineering, Maulana Azad University, Jodhpur, India*

Abstract

The emergence of mm-Wave 5G technologies necessitates the development of antenna systems capable of meeting high-frequency operational demands. This research introduces two novel antenna designs tailored for mm-Wave 5G applications, enhancing wireless communication and connectivity. Antenna Design #1 is a compact, high-efficiency patch antenna measuring 4mm × 2.75mm × 0.035mm. It features rectangular and circular slots, utilizing an inset feed technique. Operating at 31 GHz, it achieves a low return loss of -31.13 dB, a Voltage Standing Wave Ratio (VSWR) of 1.0571, and a peak gain of 5.13 dBi, making it ideal for the LMDS spectrum and 32 GHz backhaul connectivity. Antenna Design #2 builds on the first, with a slightly larger structure at 4.25mm × 2.75mm × 0.035mm, incorporating two additional rectangular slots and direct feeding via a microstrip line. This design supports dual-band operation at 28.94 GHz and 41.5 GHz, with return losses of -22 dB and -25.53 dB, and gains of 5.29 dBi and 7.31 dBi, respectively. Both designs feature broad scanning ranges in their radiation patterns, making them suitable for various 5G frequency bands, including n257 and n259. These antenna designs offer versatile, high-performance solutions for 5G network implementation, promising improvements in network coverage, capacity, and performance, and addressing the challenges posed by high-frequency 5G signals. This research lays the groundwork for future advancements in wireless communication infrastructure.

Keywords:

Patch Antenna, 5G, HFSS, mm-Wave

1. INTRODUCTION

In the era of unprecedented digital connectivity and data-driven communication, the development of advanced wireless systems has become paramount. The advent of 5G technology has redefined the landscape of wireless communication, promising higher data rates, lower latency, and enhanced connectivity for a diverse range of applications [1-2]. The fifth-generation (5G) wireless systems mark a paradigm shift in the way we perceive and experience wireless communication. While the previous generations focused predominantly on voice and data communication, 5G systems extend their capabilities to encompass the Internet of Things (IoT), virtual reality, augmented reality, autonomous vehicles, and other emerging technologies [3-4]. This transformation requires a substantial increase in data rates and a significant reduction in latency, both of which are heavily reliant on the efficient utilization of frequency spectrum.

To address the diverse demands of 5G applications, regulatory bodies and industry stakeholders have allocated multiple frequency bands spanning from sub-6 GHz to millimeter-wave (mmWave) frequencies. These include the low-band, mid-band, and high-band frequency ranges. The low-band (600 MHz - 2.7 GHz) offers wide coverage and reliable signal propagation, while the mid-band (2.7 GHz - 24 GHz) strikes a balance between coverage and capacity. The high-band or mmWave frequencies (24 GHz and above) provide immense data-carrying capabilities but require sophisticated beamforming techniques due to their susceptibility to atmospheric absorption and blockage [5-7].

In 1998, the (Federal Communications Commission) FCC introduced the Local Multipoint Distribution Service (LMDS) band via Auction 17, reserving licensed spectrum for high-speed wireless data connections, often referred to as "wireless fiber." This band, along with other millimetre wave spectrum, serves various purposes including small-cell and mobile backhaul deployments, last-mile broadband access, and emerging technologies. It's currently used by national carriers, innovative wireless companies, and regional telecom firms for high-speed fixed data networks. The LMDS band plan consists of the A Block and B Block as shown in fig. 1, each divided into two sub-band channels. A Block has A2 and A3 channels (150 MHz each), totalling 300 MHz, while B Block offers B1 and B2 channels (75 MHz each), totalling 150 MHz. Initially, there was an A1 sub-band channel with 850 MHz of spectrum in the 28 GHz range (27.500 – 28.350 GHz). Due to demand for more microwave spectrum, especially for 5G applications needing high bandwidth (> 1.0 Gbps) and low latency, the FCC reassigned the A1 channel to the new Upper Microwave Flexible Use License (UMFUS) [8-12].

At WRC-19, discussions centered around critical aspects of 5G transport networks, including the need for increased backhaul capacity. As 5G advances, repurposing current microwave frequency bands like 26GHz and 28GHz for 5G access networks becomes crucial [13-14]. Despite potential conflicts, national spectrum management can address these challenges effectively. A prime example is the 32GHz band (31.8GHz to 33.4GHz), which, while considered for 5G mobile access networks at WRC-19, is also positioned as a replacement for microwave backhaul, particularly for the 26GHz and 28GHz bands. This positioning makes it a strong contender as a global backhaul band. Apart from these bands other frequency bands like 24GHz, 37/39 GHz bands also play a pivotal role in the 5G implementations under the new UMFUS guidelines [15-16]. In future other higher mmWave bands like 37-43.5GHz, 64-71Ghz etc. may also be included/auctioned [17]. The global spectrum which are allocate or will be allocated in future for 5G deployments are shown in Table 1 [17].

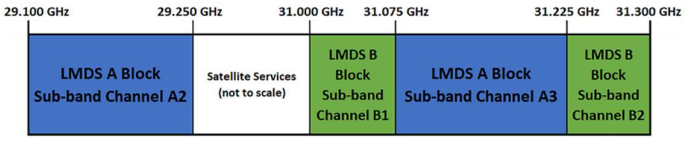

Fig. 1 The local multipoint distribution service (LMDS) frequency spectrum

Numerous research endeavours have been undertaken to design and analyse antennas capable of operating across the multi-band spectrum allocated for 5G applications. A comprehensive review of the existing literature reveals a variety of approaches and methodologies employed in the pursuit of optimal antenna designs [18-21]. Some studies focus on designing separate antennas for each frequency band, while others explore integrated solutions to cover a

wider range of frequencies [22-25]. Additionally, the incorporation of advanced materials, such as metamaterials and frequency-selective surfaces, has been explored to enhance antenna performance in terms of bandwidth, gain, and directivity [26-31].

Table 1: Global frequency spectrum allocation or targeted allocation for mm-wave 5G deployments [17]

Country	24-30GHz	37-50GHz	64-71GHz	>95GHz
United States	24.25-24.45GHz, 24.75-25.25GHz, 27.5-28.35GHz	37-37.6GHz, 37.6-40GHz, 47.2-48.2GHz, 57-64GHz		>95GHz
Canada	24.25-27.5GHz	37-37.6GHz, 37.6-40GHz		
United Kingdom	26GHz			
Germany	26GHz			
Italy	26GHz			
France	26GHz			
China	24.75-27.5GHz	40-43.5GHz		
South Korea	25.7-28.9GHz	37-38.7GHz		
Japan	26.6GHz, 27-29.5GHz	39-43.5GHz		
India	24.25-27.5GHz	37-43.5GHz		

Several research works have emphasized the significance of the microstrip patch antenna in enabling multi-band communication for 5G networks. By exploiting its inherent ability to support multiple resonances, microstrip patch antennas have demonstrated potential in achieving the desired frequency coverage while maintaining a compact and low-profile form factor. However, challenges persist in terms of achieving optimal impedance matching, radiation efficiency, and beam steering across the entire frequency spectrum. This research paper aims to contribute to the body of knowledge in this field by presenting the design and analysis of a novel microstrip patch antenna tailored for 5G applications. The proposed antenna seeks to address the aforementioned challenges and achieve efficient, reliable, and seamless communication across the diverse frequency bands mandated by 5G systems.

The subsequent sections of this paper are organized as follows: Section 2 outlines the methodology employed in the design of the preliminary antenna design #1. Section 3 presents the simulation results, performance evaluation and discussion of the antenna #1 and subsequently discusses how the preliminary design can be modified to attain dual band and hence, proposes antenna design #2. Finally, Section 4 concludes the paper.

2. Proposed Antenna Design Procedure

Rectangular patch antennas stand as one of the most extensively researched and commonly employed configurations. This study delves into variations of rectangular patch antennas, investigating diverse slot patterns. Specifically, we present two distinct designs featuring varied dimensions and slot arrangements.

At first, an equation-based design is employed to create a single-element rectangular microstrip patch antenna (MPA) for operation in the 31 GHz band. Following that, a simulation is conducted to validate the results against the defined criteria. The microstrip patch antenna is then optimized for improved performance.

2.1 Equation Based Antenna Design

The proposed antenna design #1 is built on a rectangular substrate of FR4 material with length of 6.2mm, width of 7.4mm and thickness of 1mm. The relative dielectric permittivity ε_r of the material is 4.4 and dielectric loss tangent of 0.02. From the numerous feeding techniques for microstrip patch antennas, inset feeding technique is opted to achieve effective impedance matching between the radiating patch and the feed line.

To determine the antenna's dimensions, equations (1-5) are employed. The patch's width is derived as follows:

$$w = \frac{c}{2f_r}\sqrt{\frac{2}{\varepsilon_r+1}} = \frac{3\times10^8}{2\times31\times10^9}\sqrt{\frac{2}{4.4+1}} = 0.0048\sqrt{\frac{2}{5.4}} = 2.921mm \quad (1)$$

Where, c=3×10^8m/s,

f_r=resonance frequency=31GHz

ε_r=Dielectric constant of the subsrate=4.4

To determine the length of the radiating element, it is necessary to compute the effective permittivity (ε_{eff}) of the substrate, which is determined through the following relationship:

$$\varepsilon_{eff} = \frac{\varepsilon_r+1}{2} + \frac{\varepsilon_r-1}{2\sqrt{1+12\frac{h}{w}}} = \frac{4.4+1}{2} + \frac{4.4-1}{2\sqrt{1+12\frac{1}{2.921}}} = \frac{5.4}{2} + \frac{3.4}{2\sqrt{1+0.3423}} = 2.7 + 1.2664 = 3.9664 \quad (2)$$

For a given resonance frequency f_r, the length is given by,

$$L = \frac{c}{2f_r\sqrt{\varepsilon_{eff}}} = \frac{3\times10^8}{2\times31\times10^9\sqrt{3.9664}} = \frac{3}{620\times1.9915} = 0.002429m = 2.429mm \quad (3)$$

Table 2: Derived dimension of Antenna using Equation

Parameter	Value
Frequency	31GHz
Height of the dielectric substrate, h	1mm
Dielectric Constant, ε_r	4.4
Length of the Patch, L	2.429mm
Width of the patch, w	2.921mm

However, when the antenna is designed and simulated in HFSS simulation software using the above dimensions, the results obtained were not satisfactory. Hence, the design is modified and optimized to achieve the desired results. The geometrical structure of the proposed slotted patch design is shown in fig. 2 and

dimensions are outlined in Table 3.

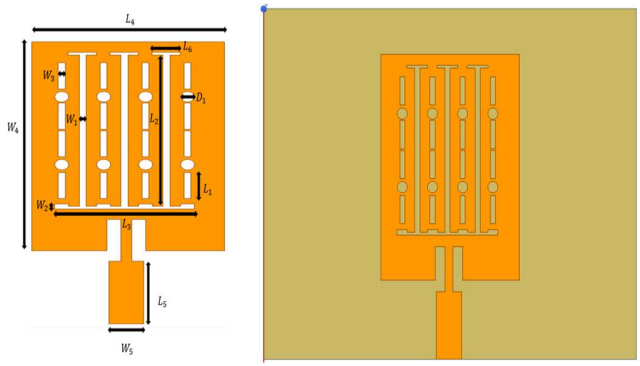

(a) **(b)**

Fig. 2 (a) Geometrical structure of the patch and the slots of the antenna design 1 (b) Top view of the antenna design 1

Table-2: Dimensions of the patch antenna design #1

Dimension	Value (in mm)
L_1	0.5
L_2	2.9
L_3	2
L_4	2.75
L_5	1.2
L_6	0.41
D_1	0.2
W_1	0.1
W_2	0.1
W_3	0.1
W_4	4
W_5	0.5

3. RESULTS AND DISCUSSION

This section delves into the analysis of both the proposed patch antenna's performance, presenting and discussing numerical findings. The focus lies on scrutinizing return loss and radiation patterns of the antenna. This evaluation is carried out using the Ansys HFSS software, a commercially accessible tool.

3.1 Result analysis of the proposed Antenna Design #1

3.1.1 Reflection Coefficient

The initial reflection coefficient value is considered as 10 dB, indicating 10% power reflection while 90% powers the antenna, ideal for mobile communication. The proposed antenna resonates at 31 GHz, showing a reflection loss of 31.12 dB as shown in fig. 3. S11 parameter is obtained via edge port power. The antenna operates within a 4.29 GHz bandwidth, equating to a relative bandwidth of 13.83%. The utilization of an inset feed power supply leads to enhanced impedance matching, resulting in a reduced reflection factor precisely at the resonance frequency.

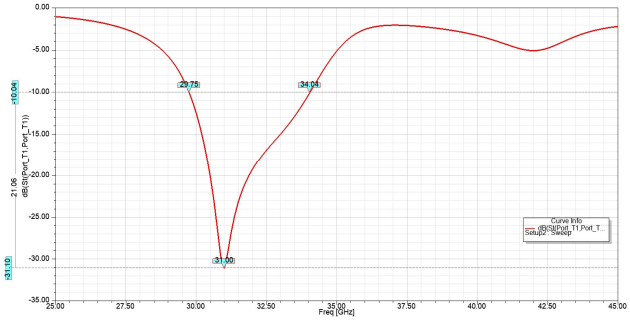

Fig. 3 Reflection Coefficient of the proposed antenna

3.1.2 Voltage Standing Wave Ratio

For a patch antenna, maintaining a voltage standing wave ratio (VSWR) below 2 across the frequency band is crucial. Ideally, the VSWR should be 1 [32]. Figure 4 depicts the VSWR across frequencies. At the 31.00 GHz resonance, VSWR is 1.0571, while it's 2 at 29.69GHz and 34.13GHz. These results confirm the antenna's operation within the frequency range (29.69 to 34.13 GHz, which falls within the LMDS frequency band).

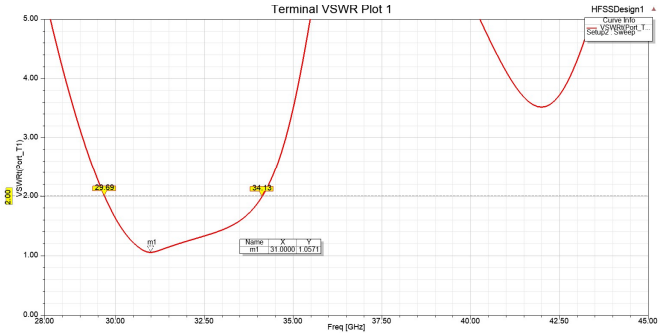

Fig. 4 VSWR vs. Frequency Chart for the Proposed 5G Antenna Design #1.

3.1.3 Input Impedance

The antenna is designed with a targeted power line impedance of 50Ω. While deviations might call for a matching system, this introduces extra losses and costs. At the resonance frequency (31.00 GHz), the feed line's complex input impedance is 47.31+ j0.29Ω. At 29.75 GHz, it's 26.16+j0.83Ω, and at 34.04 GHz, it's 27.84+j10.20 Ω. Figure 5 offers detailed input impedance values across frequencies for the proposed antenna design.

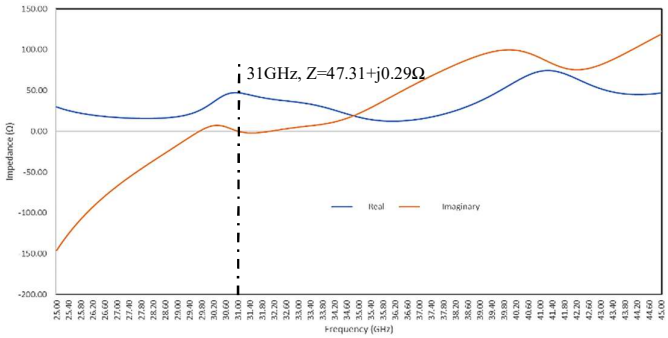

Fig. 5 Complex Input Impedance vs. Frequency for the Proposed 5G Antenna Design (Real Part in Blue, Imaginary Part in

Orange)

3.1.4 Current Distribution

In a microstrip antenna, minimal current exists at the radiating element's end, causing a phase shift between voltage and current. Consequently, the patch's edge experiences peak voltage and near-zero current values. This phenomenon is mirrored in the middle of the wave, specifically at the patch's beginning. These phase-shifted voltage and current distributions lead to distinctive field patterns at the antenna edges. Figure 6 illustrates the current distribution for frequencies 29.79 GHz (a), 34.04 GHz (b), and 31 GHz (c)

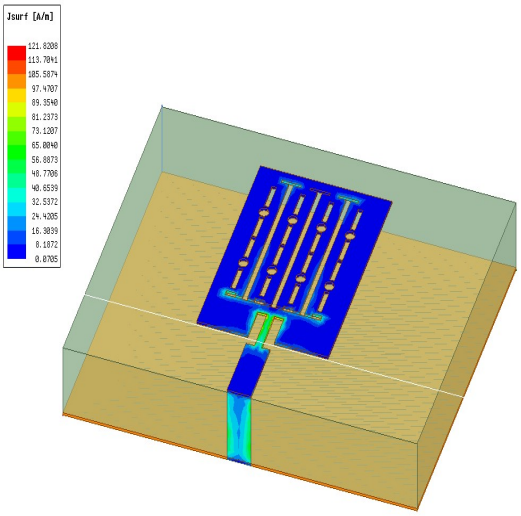

(a)

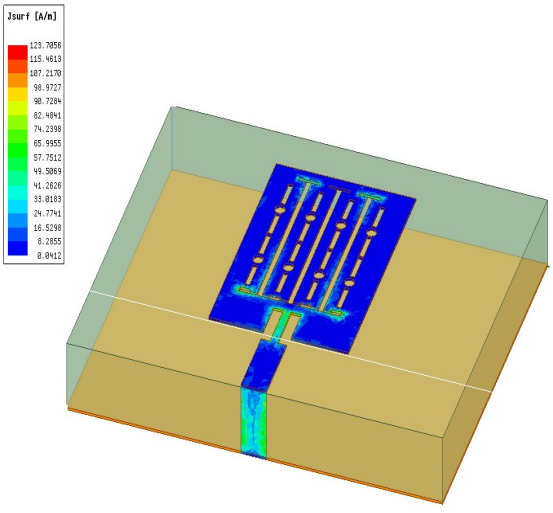

(b)

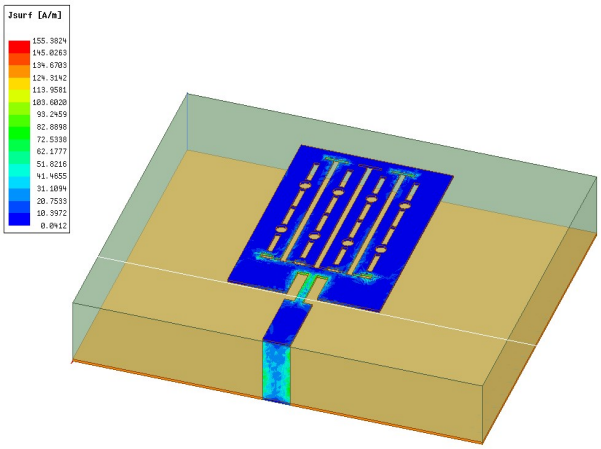

(c)

Fig. 6 Surface current distribution: (a) 29.79 GHz, (b) 34.04 GHz, (c) 31 GHz.

3.1.5 Radiation Characteristics

The radiation characteristics illustrate how the antenna emits energy in different directions, represented by standardized electric field or surface power density distributions. These traits are defined in E and H planes. The desired antenna design seeks directional radiation behaviour. Figure 7 presents the normalized radiation traits for E and H polarization, denoting the resonant frequency (31GHz) with corresponding-coloured lines.

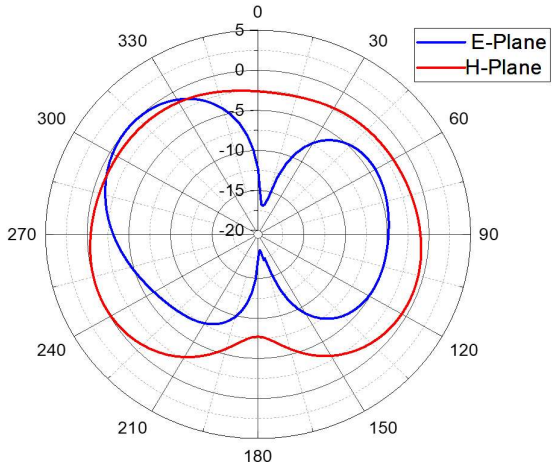

(a)

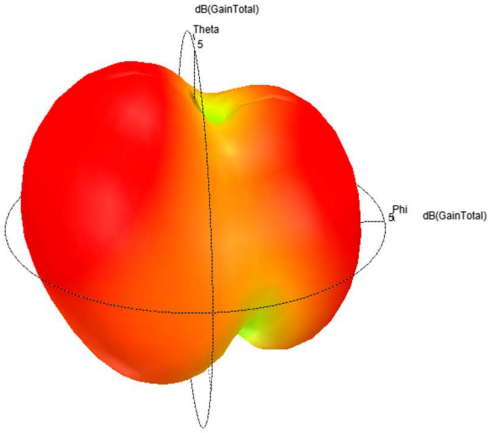

(b)

Fig. 7 (a) Normalized Radiation pattern at 31 GHz-E-plane and H-Plane. (b) 3D Radiation pattern

3.1.6 Effect of Patch length and Width

The impact of varying patch length and width on antenna performance and resonance across different frequencies was investigated. In fig. 8, which illustrates S11 plots for various patch dimensions, it's observed that the dimensions previously discussed in the paper are optimal for achieving resonance at 31GHz. Interestingly, with slight dimension adjustments, the proposed design can also facilitate dual-band operation. For instance, by setting the patch length and width to 4.25mm and 2.75mm, respectively, the antenna can effectively function at frequencies of 28.94GHz and 41.5GHz.

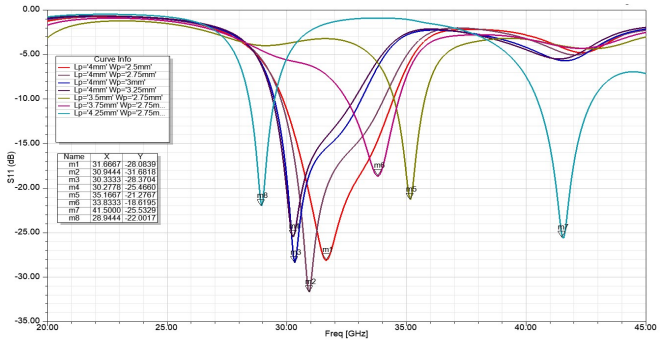

Fig. 8 Impact of patch length and width on reflection coefficient.

3.2 Modified and Optimized Design for Dual Band Patch Antenna Design #2

Upon a comprehensive evaluation of the antenna design proposed and elucidated in Section 2, a meticulous examination of the influence of patch length and width is carried out, as explained in Section 3.1.6. The outcome of this rigorous analysis reveals that marginal modifications to the patch dimensions and design bestow upon the proposed antenna the capability to operate proficiently within dual bands. The optimized dimensions for the dual-band antenna are listed in Table 4 and modified antenna design is illustrated in fig. 9. Comparing the antenna design shown in fig. 1 and the modified dual band antenna shown in fig. 9 it is seen that two slots of length (L_s) 0.8mm and width (W_s) 0.2mm are introduced in the patch, the length of the patch (L_p) is increased to 4.25mm and instead of using inset feeding a simple line feeding is utilized of length (L_f) 1.15mm and width (W_f) of 0.5mm.

Table 4. Dimensions of the dual band patch antenna

Dimension	Value (in mm)
L_1	0.5
L_2	2.9
L_3	2
L_p	4.25
Lf	1.15
Ls	0.8
D_1	0.2
W_1	0.1
W_2	2
W_3	0.41
W_p	2.75
W_f	0.5
W_s	0.2

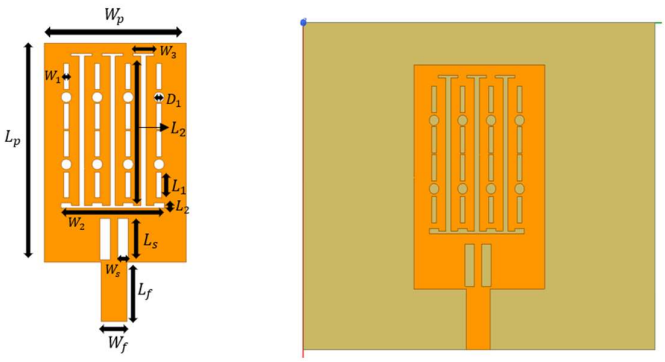

(a) (b)

Fig. 9 (a) Geometrical structure of the patch and the slots of the dual band antenna (b) Top view of the dual band antenna design #2

3.2.1 Reflection Coefficient

The initial reflection coefficient value is considered as 10 dB, indicating 10% power reflection while 90% powers the antenna, ideal for mobile communication. The modified antenna design resonates at 28.94 GHz and 41.50GHz, showing a reflection loss of 22.00 dB and 25.53dB respectively as shown in fig. 10. S11 parameter is obtained via edge port power. The antenna operates within a 1.07 GHz and 2.34GHz bandwidth for the respective bands, equating to a relative bandwidth of 3.69% and 5.6% respectively.

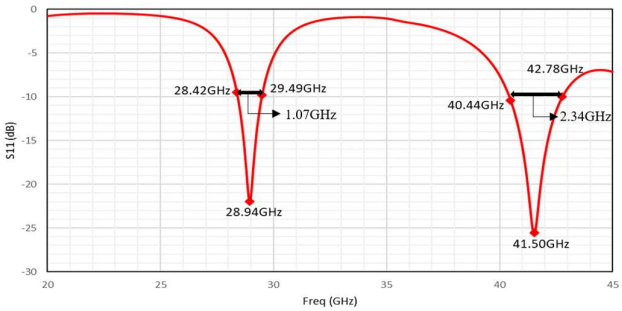

Fig. 10 Reflection Coefficient vs. Frequency for the Dual band Antenna Design

3.2.2 Voltage Standing Wave Ratio

For a patch antenna, maintaining a voltage standing wave ratio (VSWR) below 2 across the frequency band is crucial. Ideally, the VSWR should be. Figure 11 depicts the VSWR across frequencies. At the 28.94 GHz resonance, VSWR is 1.662, while it's 2 at 28.37GHz and 29.41GHz. Similarly, at the resonant frequency 41.5GHz, VSWR is 1.068, while it's 2 at 40.38GHz and 42.94GHz respectively. These results confirm the antenna's operation within the frequency range (28.37 GHz to 29.41 GHz, which falls within the n257 band commonly known as LMDS frequency band and 40.38GHz to 42.94GHz, which falls within n259 band commonly known as V frequency band).

Fig. 11 VSWR vs. Frequency Chart for the Dual band Patch Antenna Design

3.2.3 Input Impedance

The antenna is designed with a targeted power line impedance of 50Ω. While deviations might call for a matching system, this introduces extra losses and costs. At the resonance frequency (28.94 GHz and 41.50GHz), the feed line's complex input impedance is 56.79+ j4.59Ω and 45.19-j0.39 Ω respectively. Figure 12 offers detailed input impedance values across frequencies for the proposed antenna design.

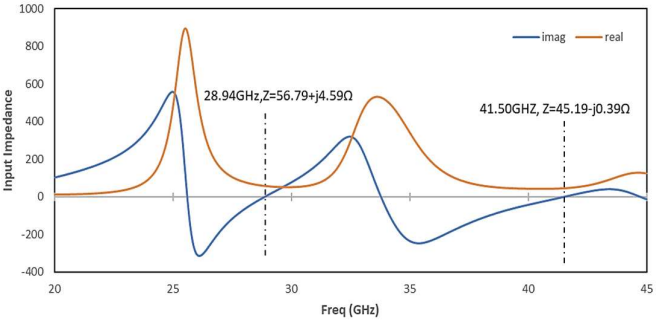

Fig. 12 Complex Input Impedance vs. Frequency for the Dual band Patch Antenna (Real Part in Orange, Imaginary Part in Blue)

3.2.5 Current Distribution

In a microstrip antenna, there is a unique current distribution along the radiating element. At the very end of the radiating element, the current is minimal, resulting in a noticeable phase difference between the voltage and current. As a consequence, the edge of the antenna patch experiences the highest voltage levels while having nearly negligible current. This phase-shifted voltage and current distribution phenomenon is also observed towards the centre of the wave, particularly at the beginning of the patch. These distinctive phase relationships between voltage and current give rise to specific field patterns at the edges of the antenna. Figure 13 illustrates this current distribution for two different frequencies: 28.94 GHz (a) and 41.5 GHz (b).

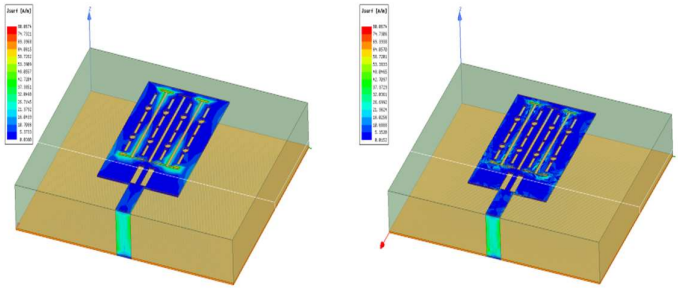

Fig. 13 Surface current distribution:(a) 28.94 GHz,(b) 41.5GHz.

3.2.6 Radiation Characteristics

Radiation characteristics show how an antenna emits energy in various directions, using standardized electric field or surface power density distributions, typically described in E and H planes. Antenna designers often aim for directional radiation. Figure 14 displays these normalized radiation traits for E and H polarization, highlighting resonant frequencies (28.94 GHz and 41.5 GHz). This visual representation helps understand antenna performance at the specific frequencies.

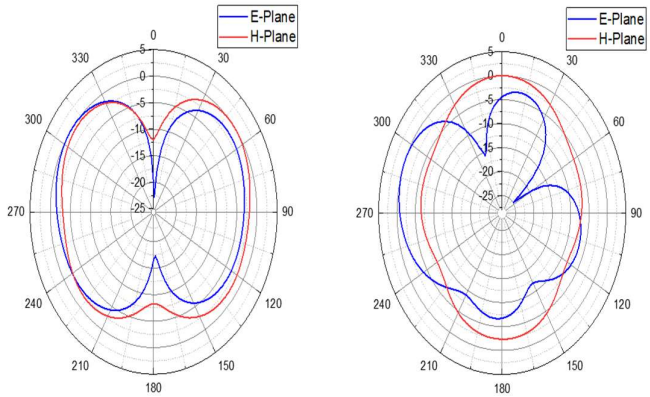

(a) (b)

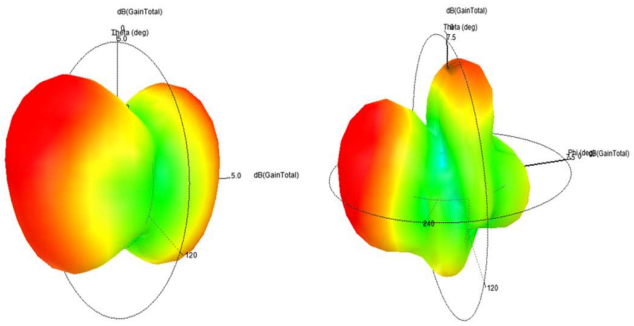

(c) (d)

Fig. 14 Radiation characteristics (E-plane and H-plane) at (a) 28.94 GHz (b) 41.5 GHz

3.2.7 Comparative Analysis

Table 5 presents a comprehensive comparison between the newly proposed antenna designs labelled as 1 and 2 and prior studies predominantly focused on operating within the mmWave frequency range, specifically spanning from 26GHz to 50GHz. The table highlights that the newly proposed antenna designs exhibit remarkable compactness while maintaining a bandwidth of operation that is comparable to few existing designs and better than few designs. Furthermore, our current design demonstrates outstanding performance in metrics such as return loss and peak gain, consistently outperforming most previous studies.

Table 5 Comparison of proposed works with previous works

Ref.	Antenna Size	Mode	Operating Frequency (GHz)	Return Loss (dB)	Peak Gain (dBi)
33	$24mm \times 24mm \times 0.203mm$	Multi-Band	26.9GHz, 29.6GHz, 31GHz, 43GHz	-22.5, -24, -20.5, -41	7.2, 6.6, 10.1, 7.1
34	$6.2mm \times 8.4mm \times 1.57mm$	Single Band	28GHz	-22.51	3.6
35	$12mm \times 12mm \times 0.237mm$	Dual Band	28.4, 37.9	-28.1, -43.8	4.5, 4.2
36	$14mm \times 12mm$	Dual Band	28, 38	-22, -15	1.27, 1.83
37	$3.054mm \times 4.235mm \times 0.8mm$	Dual Band	32, 38	-23.6	6.27, 4.73
Proposed Design #1	$4mm \times 2.75mm \times 0.035mm$	Single Band	31	-31.12	5.12
Proposed Design #2	$4.25mm \times 2.75mm \times 0.035mm$	Dual Band	28.94, 41.5	-22, -25.53	5.29, 7.31

4. Conclusion

In this paper two distinct antenna designs, labelled as Antenna Design #1 and Antenna Design #2, each with its own set of characteristics and capabilities are proposed. Antenna Design #1 was conceived with a compact design, tailored for efficient operation at 31 GHz, within a bandwidth spanning 4.29 GHz (29.69-34.13 GHz). Employing circular and rectangular slots, and incorporating inset feeding for precise input impedance matching, this antenna design delivered remarkable results. It exhibited a low return loss of 31.13 dB at its resonant frequency, VSWR of 1.0571, and achieved a peak gain of 5.13 dBi. Notably, the broad bandwidth of Antenna Design #1 positions it as a viable choice for 5G applications requiring connectivity in the 32 GHz band, particularly in backhaul scenarios. Expanding on the foundation laid by Antenna Design #1, we further modified it to introduce Antenna Design #2. This modified iteration was engineered to operate in dual bands, namely 28.94 GHz and 41.5 GHz. Simulations demonstrated that Antenna Design #2 delivered a bandwidth of approximately 1.27 GHz at 28.94 GHz and 2.34 GHz at 41.5 GHz, underscoring its versatility. The return loss values were optimized, measuring at 22 dB and 25.53 dB for 28.94 GHz and 41.5 GHz, respectively. Furthermore, Antenna Design #2 exhibited maximum gains of 5.29 dBi at 28.94 GHz and an impressive 7.31 dBi at 41.5 GHz. Thus, this work has yielded two antenna designs that hold significant promise in meeting the demands of various frequency bands. Antenna Design #1, with its generous bandwidth, is well-suited for the LMDS frequency spectrum and 32GHz backhaul connectivity band, while Antenna Design #2, capable of dual-band operation, offers flexibility for deployment in the 28-28.9 GHz and/or 37-43.5 GHz frequency bands. The frequency band 37-43.5 GHz are already auctioned in countries like Japan, China and will be auctioned in India soon. These findings underscore the potential for these antenna designs to contribute significantly to the wireless communication and connectivity specifically for the 5G applications.

.

REFERENCES

[1] Attaran M., 2023, The impact of 5G on the evolution of intelligent automation and industry digitization, J Ambient Intell Human Comput, 14, 5977–5993. https://doi.org/10.1007/s12652-020-02521-x

[2] Deepender, Manoj, Shrivastava U. and Verma K. J., 2021, A Study on 5G Technology and Its Applications in Telecommunications, 2021 International Conference on Computational Performance Evaluation (ComPE), Shillong, India, pp. 365-371, doi: 10.1109/ComPE53109.2021.9752402.

[3] Liu S., Liu L., Yang H., Yue K. and Guo T., 2020, Research on 5G technology based on Internet of things, 2020 IEEE 5th Information Technology and Mechatronics Engineering Conference (ITOEC), Chongqing, China, , pp. 1821-1823, doi: 10.1109/ITOEC49072.2020.9141671.

[4] Raman R., Alanya-Beltran J., Singh R., Trivedi S., Pillai B. G. and Chakravarthi M. K., 2023, Analysis of future trend and opportunity in the emerging 5G IoT scenario, 3rd International Conference on Advance Computing and Innovative Technologies in Engineering (ICACITE), Greater Noida, India, 2023, pp. 882-887, doi: 10.1109/ICACITE57410.2023.10183129.

[5] Dilli R., 2020, Analysis of 5G Wireless Systems in FR1 and FR2 Frequency Bands, 2020 2nd International Conference on Innovative Mechanisms for Industry Applications (ICIMIA), Bangalore, India, pp. 767-772, doi: 10.1109/ICIMIA48430.2020.9074973.

[6] Naqvi I. S., Hussain N., Alimi A., Popoola J. J., 2022, Antennas for 5G and 6G Communications, Ch. 9, IntechOpen, 10.5772/intechopen.105497

[7] 5G Spectrum-Public Policy Position, https://www-file.huawei.com/-/media/CORPORATE/PDF/public-

policy/public_policy_position_5g_spectrum.pdf

[8] Krishna C.M., et.al., 2023. High Gain Hexaport Millimetre Wave MIMO Antenna for 5G Service LMDS and N257 Band Applications. In: Nagaria, R.K., Tripathi, V.S., Zamarreno, C.R., Prajapati, Y.K. (eds) VLSI, Communication and Signal Processing. VCAS, Lecture Notes in Electrical Engineering, vol 1024. Springer, Singapore. https://doi.org/10.1007/978-981-99-0973-5_39

[9] Taghian F., Abdipour A., Mohammadi A., Roodaki P.M., Mohammadi A., 2011 Design and nonlinear analysis of a dual-band Doherty power amplifier for ISM and LMDS applications. In Proceedings of the 2011 IEEE Applied Electromagnetics Conference (AEMC), Kolkata, India, 18–22 December 2011; pp. 1–4.

[10] Resende U.C., Moreira F.J.S., Bergmann J.R., 2009, Analysis of omnidirectional antennas with radome operating in LMDS band for signals of digital TV. In Proceedings of the 2009 SBMO/IEEE MTT-S International Microwave and Optoelectronics Conference (IMOC), Belem, Brazil, 3–6 November 2009; pp. 83–86.

[11] Son L.T., Ekman T., Orten P., 2006, Performance of the multi-carrier LMDS system at the 28 GHz radio frequency band. In Proceedings of the 2006 First Mobile Computing and Wireless Communication International Conference, Amman, Jordan, 17–20 September 2006; pp. 150–155.

[12] Wireless Spectrum Licenses in the 28 GHz Band Ideal for 5G mmWave Fixed/Mobile Wireless Deployments Inquire for Details Regarding Availability, Select Spectrum, March 2020,https://www.selectspectrum.com/assets/documents/pdf/millimeter-wave/28%20GHz_Spectrum%20Summary_200330.pdf

[13] Frieden Rob, 2019, WRC-19 and 5G Spectrum Planning. TPRC47: The 47th Research Conference on Communication, Information and Internet Policy 2019, Available at SSRN: https://ssrn.com/abstract=3426175

[14] European Parliament (2019). Policy Department for Economic, Scientific and Quality of Life Policies, Directorate-General for Internal Policies. 5G Deployment, State of Play in Europe, USA and Asia. Retrieved from:

[15]https://www.europarl.europa.eu/RegData/etudes/IDAN/2019/631060/IPOL_IDA(2019)631060_EN.pdf.

[16] FCC (2019). The FCC's 5G FAST Plan. Washington, D.C.: Federal Communications Commission. Retrieved from: https://www.fcc.gov/5G

[17] FCC (2019). FCC Takes Steps to Make Millimeter Wave Spectrum Available for 5G. Retrieved from: https://docs.fcc.gov/public/attachments/FCC-19-30A1.pdf

[18] Dean B., Global 5G spectrum update, SVP, Spectrum Strategy & Technology Poilcy, Qualcomm, June 2020, Retrieved: https://www.qualcomm.com/content/dam/qcomm-martech/dm-assets/documents/20200625_mipi_-_5g_spectrum_-_dean_brenner_4.pdf

[19] Kumar S., Dixit A. S., Malekar R. R., Raut H. D. and Shevada L. K., 2020, Fifth Generation Antennas: A Comprehensive Review of Design and Performance Enhancement Techniques, IEEE Access, vol. 8, pp. 163568-163593, , doi: 10.1109/ACCESS.2020.3020952.

[20] Thakur V., Jaglan N. and Gupta S. D., 2020, A Review on Antenna Design for 5G Applications, 2020 6th International Conference on Signal Processing and Communication (ICSC), Noida, India, pp. 266-271, doi: 10.1109/ICSC48311.2020.9182774.

[21] Ruchi R., Upadhyaya P. and Dutt S., 2021, 5G Antenna at Millimeter Wave Frequency, 2021 3rd International Conference on Advances in Computing, Communication Control and Networking (ICAC3N), Greater Noida, India, pp. 1036-1038, doi: 10.1109/ICAC3N53548.2021.9725701.

[22] Parveen, K., Sabir, M., Kumari, M., Goar, V. (2019). A Slotted Microstrip Patch Antenna for 5G Mobile Phone Applications. In: Tiwari, S., Trivedi, M., Mishra, K., Misra, A., Kumar, K. (eds) Smart Innovations in Communication and Computational Sciences. Advances in Intelligent Systems and Computing, vol 851. Springer, Singapore. https://doi.org/10.1007/978-981-13-2414-7_17

[23] Yin J., Wu Q., Yu C., Wang H. and Hong W., 2019, Broadband Symmetrical E-Shaped Patch Antenna With Multimode Resonance for 5G Millimeter-Wave Applications, IEEE Transactions on Antennas and Propagation, vol. 67, no. 7, pp. 4474-4483, July 2019, doi: 10.1109/TAP.2019.2911266.

[24] Raheel K., Altaf A., Waheed A., Kiani S.H., Sehrai D.A., Tubbal F., Raad R., 2021, E-Shaped H-Slotted Dual Band mmWave Antenna for 5G Technology. Electronics, 10, 1019. https://doi.org/10.3390/electronics10091019

[25] Tang S., Chiu C.Y. and Murch R., 2022, A Millimeter-Wave Tri-Modal Patch Antenna, IEEE Antennas and Wireless Propagation Letters, vol. 21, no. 2, pp. 406-410, Feb. 2022, doi: 10.1109/LAWP.2021.3133689.

[26] Mohan M. P., Jimeno J. M., Mei S., Alphones A., Siyal M. Y. and Karim M. F., 2023, Wideband Matching Circuit for mmWave Series Fed Patch Array Antenna, IEEE Access, vol. 11, pp. 62565-62573, 2023, doi: 10.1109/ACCESS.2023.3284558.

[27] Kumar S., Singh H., 2022, A Comprehensive Review of Metamaterials/Metasurface-Based MIMO Antenna Array for 5G Millimeter-Wave Applications. J Supercond Nov Magn 35, 3025–3049. https://doi.org/10.1007/s10948-022-06408-0

[28] Moussa F. Z., Ferouani S., Belhadef Y. and Abdellaoui G., 2021, New design of miniature rectangular patch antenna with DGS for 5G mobile communications, 2021 International Conference on Information Systems and Advanced Technologies (ICISAT), Tebessa, Algeria, 2021, pp. 1-5, doi: 10.1109/ICISAT54145.2021.9678464.

[29] Esmail B. A. F. and Koziel S., 2023, Design and Optimization of Metamaterial-Based Dual-Band 28/38 GHz 5G MIMO Antenna With Modified Ground for Isolation and Bandwidth Improvement, IEEE Antennas and Wireless Propagation Letters, vol. 22, no. 5, pp. 1069-1073, May 2023, doi: 10.1109/LAWP.2022.3232622.

[30] Ahmad I., Tan W., Ali Q., Sun H., 2022, Latest Performance Improvement Strategies and Techniques Used in 5G Antenna Designing Technology, a Comprehensive Study. Micromachines, 13, 717. https://doi.org/10.3390/mi13050717

[31] Alwareth H., Ibrahim I.M., Zakaria Z., Al-Gburi A.J.A., Ahmed S., Nasser, Z.A., 2022, A Wideband High-Gain Microstrip Array Antenna Integrated with Frequency-Selective Surface for Sub-6 GHz 5G Applications. Micromachines, 13, 1215. https://doi.org/10.3390/mi13081215

[32] Singh G., Abrol A., Kumar S., Kanaujia B.K., Pandey V.K., 2023, Electromagnetic metamaterial-inspired wideband millimeter-wave antenna for 5G communication, Materials Today: Proceedings, ISSN 2214-7853, https://doi.org/10.1016/j.matpr.2023.03.464.

[33] Derneryd A., A theoretical investigation of the rectangular microstrip antenna element, IEEE Transactions on Antennas and

Propagation, vol. 26, no. 4, pp. 532-535, July 1978, doi: 10.1109/TAP.1978.1141890.

[34] El-Hakim H., Mohamed H.A., 2023, Synthesis of a Multiband Microstrip Patch Antenna for 5G Wireless Communications. J Infrared Milli Terahz Waves. https://doi.org/10.1007/s10762-023-00937-y

[35] Przesmycki R., Bugaj M., Nowosielski L., 2021, Broadband Microstrip Antenna for 5G Wireless Systems Operating at 28 GHz., Electronics, 10, https://dx.doi.org/10.3390/electronics10010001

[36] Sabek Ayman R and Ibrahim Ahmed A and Ali Wael A, 2021, Dual-Band Millimeter Wave Microstrip Patch Antenna with Stub Resonators for 28/38 GHz Applications, Journal of Physics: Conference Series, IOP Publishing, vol. 2128(1),pp. 012006, DOI: 10.1088/1742-6596/2128/1/012006

[37] Hasan M. N, Bashir S. and Chu S., 2019, Dual band omnidirectional millimeter wave antenna for 5G communications, Journal of Electromagnetic Waves and Applications, 33:12, 1581-1590, DOI: 10.1080/09205071.2019.1617790